AGU ADVANCING EARTH AND SPACE SCIENCE

Earth and Space Science

RESEARCH ARTICLE
10.1029/2021EA001763

Based on Atmospheric Physics and Ecological Principle to Assess the Accuracies of Field CO_2/H_2O Measurements From Infrared Gas Analyzers in Closed-Path Eddy-Covariance Systems

Xinhua Zhou[1,2,3,4], Tian Gao[1,2,5], Yunchao Pang[1,2,6], Hayden Mahan[3], Xiufen Li[2,5,6], Ning Zheng[2,7], Andrew E. Suyker[4], Tala Awada[4], and Jiaojun Zhu[1,2,5]

[1]CAS Key Laboratory of Forest Ecology and Management, Institute of Applied Ecology, Chinese Academy of Sciences (CAS), Shenyang, China, [2]CAS-CSI Joint Laboratory of Research and Development for Monitoring Forest Fluxes of Trace Gases and Isotope Elements, Institute of Applied Ecology, Chinese Academy of Sciences, Shenyang, China, [3]Campbell Scientific Incorporation, Logan, UT, USA, [4]School of Natural Resources, University of Nebraska, Lincoln, NE, USA, [5]Qingyuan Forest CERN, Chinese Academy of Sciences, Shenyang, China, [6]Department of Agricultural Meteorology, Shenyang Agricultural University, Shenyang, China, [7]Beijing Servirst Technology Limited, Beijing, China

Key Points:

- Paper develops accuracy equations for CO_2/H_2O measurements from infrared gas analyzers in closed-path eddy-covariance systems
- The equations are used to assess the improvement in CO_2/H_2O measurement accuracy of analyzers under automatic zero/span procedures
- Assessments find that, for analyzers in cold/dry conditions, the zero procedure is important, but the H_2O span procedure is unnecessary

Correspondence to:
T. Gao,
tiangao@iae.ac.cn

Citation:
Zhou, X., Gao, T., Pang, Y., Mahan, H., Li, X., Zheng, N., et al. (2021). Based on atmospheric physics and ecological principle to assess the accuracies of field CO_2/H_2O measurements from infrared gas analyzers in closed-path eddy-covariance systems. *Earth and Space Science*, *8*, e2021EA001763. https://doi.org/10.1029/2021EA001763

Received 24 MAR 2021
Accepted 21 SEP 2021

Abstract Field CO_2/H_2O measurements from infrared gas analyzers in closed-path eddy-covariance systems have wide applications in earth sciences. Knowledge about exactness of these measurements is required to assess measurement applicability. Although the analyzers are specified with uncertainty components (zero drift, gain drift, cross-sensitivities, and precision), exactness for individual measurements is unavailable due to an absence of methodology to comprehend the components as an overall uncertainty. Adopting an advanced definition of accuracy as a range of all measurement uncertainty sources, the specified components are composited into a model formulated for studying analyzers' CO_2/H_2O accuracy equations. Based on atmospheric physics and environmental parameters, the analyzers are evaluated using the equations for CO_2 accuracy (±0.78 $\mu molCO_2\ mol^{-1}$, relatively ±0.18%) and H_2O accuracy (±0.15 $mmolH_2O\ mol^{-1}$). Evaluation shows that precision and cross-sensitivity are minor uncertainties while zero and gain drifts are major uncertainties. Both drifts need adjusting through zero/span procedures during field maintenance. The equations provide rationales to guide and assess the procedures. H_2O span needs more attentions under humid conditions. Under freezing conditions while H_2O span is impractical, this span is fortunately unnecessary. Under the same conditions, H_2O zero drift dominates H_2O measurement uncertainty. Therefore, automatic zero becomes a more applicable and necessary tactic. In general cases of atmospheric CO_2 background, automatic CO_2 zero/span procedures can narrow CO_2 accuracy by 36% (±0.74 to ± 0.47 $\mu molCO_2\ mol^{-1}$). Automatic/manual H_2O zero/span procedures can narrow H_2O accuracy by 27% (±0.15 to ±0.11 $mmolH_2O\ mol^{-1}$). While ensuring system specifications, the procedures guided by equations improve measurement accuracies.

1. Introduction

Closed-path eddy-covariance (CPEC) systems are used to measure boundary-layer CO_2, H_2O, heat, and momentum fluxes between ecosystems and the atmosphere (Ibrom et al., 2007; Leuning & Moncrieff, 1990). For the fluxes, a CPEC system is equipped with a fast response three-dimensional (3D) sonic anemometer to measure wind and sonic temperature (T_s) and a fast-response infrared gas analyzer to measure CO_2 and H_2O amounts. In this configuration, CO_2 and H_2O are measured inside the analyzer cuvette. For both measurements, air is sampled into the cuvette from the analyzer sampling orifice adjacently positioned to the sonic measurement volume (Figure 1). Together, the anemometer and analyzer provide high-frequency (e.g., 10 Hz) measurements used to compute the fluxes (Aubinet et al., 2012) at a location represented by the sonic measurement volume and the gas analyzer orifice position. The degree of exactness of each flux from the measured data depends primarily on the exactness of field measurements for CO_2, H_2O, and/or T_s along with 3D wind (Fratini et al., 2014). Beyond the acquisition for the fluxes, the data of individual variables from these field measurements have various applications in other domains. In many settings, knowledge of measurement exactness is required for assessing data applicability. This study models and assesses this exactness of CO_2/H_2O data from the infrared gas analyzers in CPEC systems (Figure 1) used in ecosystems.

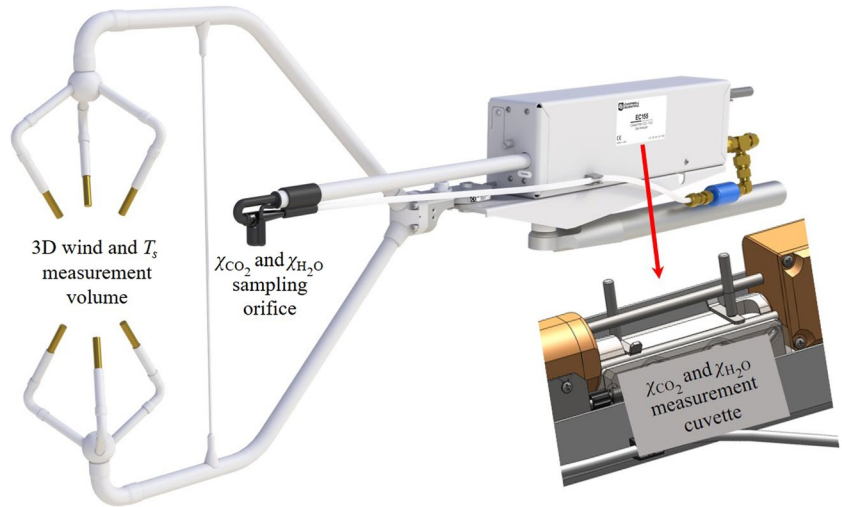

Figure 1. Sonic measurement volume for three-dimensional (3D) wind and sonic temperature (T_s), gas analyzer sampling orifice position for CO_2 mixing ratio (χ_{co_2}) and H_2O mixing ratio (χ_{H_2O}), and the gas analyzer measurement cuvette for χ_{co_2} and χ_{H_2O} in a CPEC system (e.g., CPEC310, Campbell Scientific Inc., UT, USA).

The analyzers in CPEC systems output CO_2 mixing ratio (i.e., $\chi_{CO_2} = \rho_{CO_2}/\rho_d$ where ρ_{CO_2} is CO_2 molar concentration and ρ_d is dry air molar concentration) and H_2O mixing ratio (i.e., $\chi_{H_2O} = \rho_{H_2O}/\rho_d$, where ρ_{H_2O} is H_2O molar concentration). For instance, χ_{H_2O} along with T_s can be used to derive ambient air temperature (T_a) (Kaimal & Gaynor, 1991; Schotanus et al., 1983). In this case, given an exact T_a equation, the applicability of equation relies solely on the measurement exactness of χ_{H_2O} and T_s. Therefore, the higher the degree of exactness of χ_{H_2O} and T_s, the higher the degree of exactness of T_a. The evaluation on the uncertainty of T_a from χ_{H_2O} and T_s measurements needs the overall exactness values of χ_{H_2O} and T_s. Although the uncertainty sources related to the exactness of gas analyzer measurements are separately specified by drifts, cross-sensitivities, and precision (Campbell Scientific Inc., 2018a; LI-COR Biosciences, 2016), specifications for the exactness of such individual field measurements have been unavailable until now. This is due to the absence of methodology to comprehend all individual uncertainty sources.

For any sensor, the measurement exactness depends on its performances, which are commonly specified in terms of accuracy, precision, and other uncertainty descriptors, such as sensor drift. Conveniently, the accuracy represents trueness as a systematic uncertainty to quantify the degree of closeness of measurement to the true value in a measured quantity. The precision is the standard deviation of random measurement errors to quantify the degree to which repeated measurements under unchanged conditions show the same results (Joint Committee for Guide in Metrology, 2008). Both accuracy and precision are universally applicable to any sensor for its performance specifications. Other uncertainty descriptors are more sensor specific. For example, cross-sensitivity of CO_2 measurement detection to H_2O may be applicable only to infrared gas analyzers. Overall exactness of individual measurements is comprehensively descriptive and, in practice as in the above case for T_a, is most needed by users for their data analyses. Therefore, International Organization for Standardization (2012) advanced the definition of accuracy in a comprehensive way. The accuracy was expanded in its definition as the combination of both trueness and precision. This advanced definition is advantageous and, while keeping the terminology of "accuracy," consolidates all measurement uncertainties together. Adopting this definition, we specify the accuracy of individual measurements from infrared gas analyzers as the range of total uncertainty from all individual uncertainty sources in field measurements. Using the analyzer specifications of the CPEC300 series (Campbell Scientific Inc.) as an example, we: (a) develop methodologies to comprehend all measurement uncertainty sources of infrared gas analyzers as the accuracy of CO_2/H_2O measurements into an equation, (b) assess the accuracy of CO_2/H_2O measurements using the equation, and (c) discuss applications of the assessments in data analyses and analyzer field maintenance. Additional objective of this study is to find an approach for flux community to assess the accuracy of field CO_2/H_2O measurements from infrared gas analyzers in CPEC systems.

Table 1
Measurement Specifications for EC155 Infrared CO_2/H_2O Analyzers (Campbell Scientific Inc., 2018a)

	CO_2			H_2O			
	Notation	Value	Unit	Notation	Value	Unit	Note
Precision	σ_{co_2}	0.15	$\mu molCO_2\ mol^{-1}$ [a]	σ_{H_2O}	6.0×10^{-3}	$mmolH_2O\ mol^{-1}$	
Zero drift	d_{cz}	±0.30	$\mu molCO_2\ mol^{-1}$	d_{wz}	±0.05	$mmolH_2O\ mol^{-1}$	Both zero and gain drift values are the possible maxima within the system operational range of ambient air temperature. The actual values depend more on this temperature.
Gain drift	d_{cg}	±0.10%[b] trueχ_{co_2}	$\mu molCO_2\ mol^{-1}$	d_{wg}	±0.30%[c] true χ_{H_2O}	$mmolH_2O\ mol^{-1}$	
Cross-sensitivity to H_2O	s_w	$\pm 5.6 \times 10^{-8}$	$\mu molCO_2\ mol^{-1}\ (mmolH_2O\ mol^{-1})^{-1}$		N/A		
Cross-sensitivity to CO_2		N/A		s_c	$\pm 5.0 \times 10^{-5}$	$mmolH_2O\ mol^{-1}\ (\mu molCO_2\ mol^{-1})^{-1}$	
Calibration range		0–1,000	$\mu molCO_2\ mol^{-1}$		0–79	$mmolH_2O\ mol^{-1}$	For CO_2, up to 3,000 $\mu molCO_2\ mol^{-1}$ if specially needed.

[a]mol in the denominator of all units is mole of dry air. [b]0.10% is CO_2 gain drift percentage denoted by $\delta_{co_{2\_g}}$ in text and χ_{co_2} is CO_2 molar mixing ratio. [c]0.30% is H_2O gain drift percentage denoted by $\delta_{H_2O\_g}$ in text and χ_{H_2O} is H_2O molar mixing ratio.

2. Specifications

A system of CPEC300 series includes, but is not limited to, a CSAT3A 3D sonic anemometer and an EC155 infrared CO_2/H_2O analyzer. The system operates in an ambient air temperature range of −30 to 50°C and an atmospheric pressure range of 70–106 kPa. The specifications for CO_2 and H_2O measurements are given in Table 1.

In this table, the top limit of 1,000 $\mu molCO_2\ mol^{-1}$ in the calibration range for CO_2 is more than double the background CO_2 mixing ratio in the atmosphere (415 $\mu molCO_2\ mol^{-1}$, Global Monitoring Laboratory, 2021). The top limit of 79 $mmolH_2O\ mol^{-1}$ in the calibration range for H_2O is equivalent to 40°C dew point under the atmospheric pressure of 101.325 kPa as used by Wright et al. (2003). This limit is higher than the highest dew point of 35°C ever recorded under natural conditions on Earth (National Weather Service, 2021).

The uncertainties of gas analyzers for CO_2 and H_2O measurements in Table 1 are specified by individual uncertainty sources along with their magnitudes. For CO_2 and H_2O measurements, respectively, the composite uncertainty range (i.e., the accuracy) is needed most and should be derived from these sources.

The precision uncertainty is caused by random measurement errors, and the other uncertainties can be considered as systematic uncertainties related to trueness. As noted in Table 1, zero and gain drifts are more influenced by ambient air temperature. Additionally, each gain drift is also positively proportional to its own magnitude (i.e., true χ_{CO_2} or χ_{H_2O}). Lastly, while measuring CO_2, sensitivity-to-H_2O is related to the background concentration of H_2O as indicated by its unit of $\mu molCO_2\ mol^{-1}\ (mmolH_2O\ mol^{-1})^{-1}$ and, while measuring H_2O, sensitivity-to-CO_2 is related to the background concentration of CO_2 as indicated by its unit of $mmolH_2O\ mol^{-1}\ (\mu molCO_2\ mol^{-1})^{-1}$.

Accordingly, beyond statistical analysis, the accuracy of CO_2/H_2O measurements should be evaluated in an ambient air temperature range of −30 to 50°C, a χ_{H_2O} range of 0–79 $mmolH_2O\ mol^{-1}$, and a χ_{CO_2} range up to 1,000 $\mu molCO_2\ mol^{-1}$.

3. Accuracy Model

As a maximum range of composite uncertainty, the accuracy is determined collectively by all individual uncertainty components: zero drift, gain drift, precision, and cross-sensitivity-to-α uncertainties where α can be either CO_2, if H_2O is measured, or H_2O, if CO_2 is measured. Given the true α mixing ratio ($\chi_{\alpha T}$) and measured one (χ_α), the composite uncertainty of measured α mixing ratios ($\Delta\chi_\alpha$) is given by:

$$\Delta\chi_\alpha = \chi_\alpha - \chi_{\alpha T} \tag{1}$$

The accuracy model is an expression of the maximum range of $\Delta\chi_\alpha$ in terms of quantified measurement uncertainties.

The zero drift uncertainty $\left(\Delta\chi_\alpha^z\right)$ is independent of $\chi_{\alpha T}$ in value. The cross-sensitivity uncertainty $\left(\Delta\chi_\alpha^s\right)$ is also independent of $\chi_{\alpha T}$ in value, but depends on the amount of background H_2O in the air if α is CO_2 and on the amount of background CO_2 in air if α is H_2O. Therefore, while both gain drift and precision uncertainties are zero, $\Delta\chi_\alpha^z$ and $\Delta\chi_\alpha^s$ are additive to $\chi_{\alpha T}$ as a measured value with zero drift and cross-sensitivity uncertainties (χ_{α_zs}):

$$\chi_{\alpha\_zs} = \chi_{\alpha T} + \Delta\chi_\alpha^z + \Delta\chi_\alpha^s \tag{2}$$

Along with the zero drift and the cross-sensitivity uncertainty in a measurement process, if gain also drifts, χ_{α_zs} would be a base magnitude from which gain drifts. As such, the measured value with the zero drift and cross-sensitivity uncertainties plus the gain drift uncertainty (χ_{α_zsg}) can be evaluated as:

$$\chi_{a\_zsg} = \chi_{\alpha\_zs} + \delta_{\alpha\_g}\chi_{\alpha\_zs} \tag{3}$$

where δ_{α_g} is the gain drift percentage ($\delta_{co_2\_g} = 0.10\%$ and $\delta_{H_2O\_g} = 0.30\%$, Table 1). Substituting χ_{α_zs} in this equation with Equation 2 leads to:

$$\chi_{a\_zsg} = \chi_{\alpha T} + \Delta\chi_\alpha^z + \Delta\chi_\alpha^s + \delta_{\alpha\_g}\chi_{\alpha T} + \delta_{\alpha\_g}\Delta\chi_\alpha^z + \delta_{\alpha\_g}\Delta\chi_\alpha^s \tag{4}$$

In the right side of this equation, the magnitude of $\delta_{\alpha\_g}\Delta\chi_\alpha^z$ is three orders smaller than $\Delta\chi_\alpha^z$ and the magnitude of $\delta_{\alpha\_g}\Delta\chi_\alpha^s$ is three orders smaller than $\Delta\chi_\alpha^s$. These two smaller terms can be dropped and Equation 4 can be approximated and re-arranged as:

$$\begin{aligned}\chi_{a\_zsg} &\approx \chi_{\alpha T} + \Delta\chi_\alpha^z + \delta_{\alpha\_g}\chi_{\alpha T} + \Delta\chi_\alpha^s \\ &= \chi_{\alpha T} + \Delta\chi_\alpha^z + \Delta\chi_\alpha^g + \Delta\chi_\alpha^s\end{aligned} \tag{5}$$

Any measured value has a random error (i.e., precision uncertainty) independent of $\chi_{\alpha T}$ in value that is caused by unknown minor factors (International Organization for Standardization, 2012). Therefore, the precision uncertainty is additive to any measurement. Adding this precision uncertainty ($\Delta\chi_\alpha^p$) to χ_{α_zsg} leads to a measured value (χ_α) including all uncertainties, given by:

$$\begin{aligned}\chi_a &= \chi_{a\_zsg} + \Delta\chi_\alpha^p \\ &= \chi_{\alpha T} + \Delta\chi_\alpha^z + \Delta\chi_\alpha^g + \Delta\chi_\alpha^s + \Delta\chi_\alpha^p\end{aligned} \tag{6}$$

The replacement of χ_α in Equation 1 with this equation expresses the composite uncertainty as:

$$\Delta\chi_a = \Delta\chi_\alpha^z + \Delta\chi_\alpha^s + \Delta\chi_\alpha^g + \Delta\chi_\alpha^p \tag{7}$$

$$\Delta\chi_a \le \left|\Delta\chi_\alpha^z\right| + \left|\Delta\chi_\alpha^g\right| + \left|\Delta\chi_\alpha^s\right| + \left|\Delta\chi_\alpha^p\right| \tag{8}$$

The four terms in the right side of this equation define a range of composite uncertainty for α gas species measurements as the accuracy in a model:

$$\Delta\chi_\alpha \equiv \pm\left(\left|\Delta\chi_\alpha^z\right| + \left|\Delta\chi_\alpha^g\right| + \left|\Delta\chi_\alpha^s\right| + \left|\Delta\chi_\alpha^p\right|\right) \tag{9}$$

Assessment on the accuracy of field CO_2 or H_2O measurements is to formulate and evaluate the four terms in the right side of this model. The involvement of dry air molar concentration in the expression of χ_{CO_2}

and χ_{H_2O} requires H_2O molar concentration in moist air to be known first; therefore, the accuracy of H_2O measurements is studied prior to CO_2.

4. Accuracy of H_2O Mixing Ratio Measurements

Accuracy model (9) defines the accuracy of H_2O measurements by infrared gas analyzers $\left(\Delta\chi_{H_2O}\right)$ as

$$\Delta\chi_{H_2O} \equiv \pm\left(\left|\Delta\chi^{z}_{H_2O}\right| + \left|\Delta\chi^{g}_{H_2O}\right| + \left|\Delta\chi^{s}_{H_2O}\right| + \left|\Delta\chi^{p}_{H_2O}\right|\right) \tag{10}$$

where $\Delta\chi^{z}_{H_2O}$ is H_2O zero drift uncertainty, $\Delta\chi^{g}_{H_2O}$ is H_2O gain drift uncertainty, and $\Delta\chi^{s}_{H_2O}$ is cross-sensitivity-to-CO_2 uncertainty, and $\Delta\chi^{p}_{H_2O}$ is H_2O precision uncertainty.

The H_2O precision is the standard deviation of χ_{H_2O} random errors among repeated measurements under the same conditions (International Organization for Standardization, 2012). Accordingly, the precision uncertainty in an individual H_2O measurement due to this deviation at a *P*-value of 0.05 can be defined by statistic theory (Snedecor & Cochran, 1989) as:

$$\Delta\chi^{p}_{H_2O} = \pm 1.96 \times \sigma_{H_2O} \tag{11}$$

The remaining uncertainties due to H_2O zero drift, H_2O gain drift, and cross-sensitivity-to-CO_2 are caused by the inability of the working equation inside the gas analyzers to perform consistently for a long-term (e.g., months or seasons) under varying environmental conditions such as, ambient air temperature. According to LI-Cor Biosciences (2016), a general model of the working equation for χ_{H_2O} is given by:

$$\begin{aligned}\rho_{H_2O} &= P\sum_{i=1}^{3} a_{wi}\left\{1-\left[\frac{A_w}{A_{ws}} + S_c\left(1-\frac{A_c}{A_{cs}}\right)\right]Z_w\right\}^{i}\left\{\frac{G_w}{P}\right\}^{i}\\ \chi_{H_2O} &= \rho_{H_2O}\left[\frac{P}{R^*\left(T_g+273.15\right)} - \frac{\rho_{H_2O}}{1000}\right]^{-1}\end{aligned} \tag{12}$$

where ρ_{H_2O} is H_2O molar concentration in mmolH_2O m^{-3}; a_{wi} (i = 1, 2, or 3) is a coefficient of the third order polynomial in the terms inside curly brackets; A_{ws} and A_{cs} are the power of analyzer source lights in the wavelengths for H_2O and CO_2 measurements, respectively; A_w and A_c are the portions of source light power of A_{ws} and A_{cs} that pass through the gas; S_c is cross-sensitivity of detector to CO_2, while detecting H_2O, in the wavelength for H_2O measurements (hereinafter referred as sensitivity-to-CO_2); Z_w is H_2O zero adjustment (H_2O zero coefficient); G_w is H_2O gain adjustment (i.e., H_2O gain coefficient commonly as H_2O span coefficient); P and T_g are gas pressure and gas temperature, respectively, inside the closed-cuvette; and R^* is the universal gas constant. The parameters of a_{wi}, Z_w, G_w, and S_c in this model are statistically estimated to establish a H_2O working equation in the production calibration against a series of standard gases in a range of H_2O along with CO_2 molar concentrations under a range of P (hereinafter referred as calibration). The H_2O working equation (i.e., Model [12] with estimated parameters) is used inside the gas analyzer to compute ρ_{H_2O} and χ_{H_2O} from field measurements of A_c, A_{cs}, A_w, A_{ws}, P, and T_g.

The working equation is analyzer-specific and is deemed accurate immediately after the calibration process (LI-Cor Biosciences, 2016). However, similar to all optical instruments, after being used in environments different from the manufacturer calibration conditions, an analyzer drifts in H_2O zero and/or gain. As Model (12) for ρ_{H_2O} shows, parameter Z_w is related to H_2O zero drift; G_w, to H_2O gain drift; and S_c, to sensitivity-to-CO_2. Therefore, the analyses of Z_w and G_w along with S_c are an approach to understand the causes of zero drift, gain drift, and sensitivity-to-CO_2. Such understanding is essential to formulate $\Delta\chi^{z}_{H_2O}$, $\Delta\chi^{g}_{H_2O}$, and $\Delta\chi^{s}_{H_2O}$.

4.1. Z_w and $\Delta\chi^{z}_{H_2O}$ (H_2O Zero Drift Uncertainty)

Gas analyzers are calibrated to report zero χ_{H_2O} plus the precision uncertainty for zero gas that is free of H_2O and CO_2 (hereinafter referred as zero gas). However, when used in measurement conditions that are vastly different from the calibration conditions, the analyzers often report non-zero χ_{H_2O} value for zero gas, even

beyond $\pm\Delta\chi^{p}_{H_2O}$. This instability of gas analyzers is termed as H_2O zero drift. The drift is primarily affected by air temperature surrounding the gas analyzer that is different from the ambient air temperature in the calibration processes (T_c) and/or by small H_2O accumulation inside the analyzer light housing (hereinafter referred as housing H_2O accumulation) due to unavoidable little gas leaking during long-term use. The light housing is technically sealed to keep housing air close to zero gas by using molecular sieve to remove CO_2 and H_2O from any ambient air that may sneak into the housing (Campbell Scientific Inc., 2018a).

Due to the H_2O zero drift, the working equation needs to be adjusted through its parameter re-estimation to adapt to the ambient air temperature and housing H_2O accumulation near which the system is running. This adjustment is the zero procedure to bring χ_{H_2O} and χ_{CO_2} of the zero gas from the working equation back to zero, or as close as possible. This section just focuses on H_2O instead of CO_2 for our discussion about the zero procedure. The same theory applies for CO_2.

In the field, a simple zero procedure is preferred. Since only a zero H_2O value is available, the simplest method is to use zero gas to re-estimate one parameter in the working equation that results in zero χ_{H_2O} due to zero ρ_{H_2O}. As Model (12) shows, this parameter for H_2O turns out to be Z_w adjustable to result in zero ρ_{H_2O} for zero gas if re-estimated by:

$$Z_w = \left[\frac{A_{w0}}{A_{ws}} + S_c\left(1 - \frac{A_{c0}}{A_{cs}}\right)\right]^{-1} \tag{13}$$

where A_{w0} and A_{c0} are the counterparts of A_w and A_c for zero gas, respectively. Inside the analyzer, the zero procedure for H_2O is to re-estimate the H_2O zero coefficient to satisfy Equation 13.

If the H_2O zero coefficient always satisfies Equation 13 after the zero procedure, the H_2O zero drift would not cause a significant uncertainty in H_2O measurements; however, this is not the case. Similar to the performance after the calibration, an analyzer after the zero procedure will likely drift slowly under changing ambient air temperature. Nevertheless, the value of H_2O zero coefficient that should be used with the ambient air temperature surrounding the gas analyzer, and particularly with housing H_2O accumulation, is unpredictable. Given that the molecular sieve inside the analyzer light housing is replaced as recommended in the analyzer maintenance schedule, the housing H_2O accumulation should not be a concern while the temperature surrounding the gas analyzer is not under control. Therefore, the H_2O zero drift uncertainty is specified as the maximum range of H_2O zero drift for the analyzers (d_{wz}) that varies with ambient air temperature (Campbell Scientific Inc., 2018b), but normally within the specified range.

Given that an analyzer performs best, almost without zero drift, at the same ambient air temperature as the calibration/zeroing ambient air temperature (T_c) and possibly drifts while T_g changes away from T_c. The further T_g is away from T_c, the more likely it will drift in proportion to the difference between T_g and T_c but within the specification over the analyzer operational range of ambient air temperature. Accordingly, H_2O zero drift uncertainty can be approximated for its maximum range as:

$$\Delta\chi^{z}_{H_2O} \equiv d_{wz} \times \begin{cases} \dfrac{T_g - T_c}{T_{rh} - T_{rl}} & T_c < T_g < T_{rh} \\ \dfrac{T_c - T_g}{T_{rh} - T_{rl}} & T_c > T_g > T_{rl} \end{cases} \tag{14}$$

where, over the analyzer operational range of ambient air temperature, T_{rh} is the high-end value (50°C for our study case) and T_{rl} is the low-end value (−30°C for our study case). In this equation, $\Delta\chi^{z}_{H_2O} \le d_{wz}$ over the full range of ambient air temperature from T_{rl} to T_{rh} and $\Delta\chi^{z}_{H_2O} = d_{wz}$ if T_g and T_c are at the two ends of the range (i.e., T_{rl} and T_{rh}), respectively.

4.2. G_w and $\Delta\chi^{g}_{H_2O}$ (H_2O Gain Drift Uncertainty)

All CO_2/H_2O analyzers are calibrated against a series of moist air with known H_2O molar concentrations at different levels. This calibration sets the working equation to closely follow the gain trend in H_2O change of measured moist air. Similar to the zero drift, during use with changing ambient conditions, the reported gain trend of χ_{H_2O} for H_2O changes in air will possibly drift away from the real gain trend of the change,

which is specifically termed as H_2O gain drift. This drift is affected by almost the same factors as the H_2O zero drift (LI-COR Bioscience, 2016).

Due to possible gain drift, the gas analyzer after the zero procedure needs to be further adjusted to tune its working equation back to the real gain trend in H_2O of measured air or as close as possible, which is the H_2O span procedure. Like the zero procedure, this procedure is also required to be simple using one H_2O span gas with known water density ($\tilde{\rho}_{H_2O}$), which is close to typical ambient water density values in the measurement environment. Also, because one H_2O value from H_2O span gas is used, only one parameter in the working equation can be adjusted while others are fixed. Weighing the gain of the working equation more than any other parameter, this parameter is the H_2O span coefficient (i.e., G_w) in Model (12). The H_2O span is used to re-estimate G_w to satisfy the following equation (for more details, see LI-COR Bioscience, 2016):

$$\left|\tilde{\rho}_{H_2O} - \rho_{H_2O}\left(G_w\right)\right| = \min\left|\tilde{\rho}_{H_2O} - \rho_{H_2O}\right| \tag{15}$$

After the H_2O span procedure, the H_2O gain drift can continue to occur.

Based on the similar considerations as the H_2O zero drift, the H_2O gain drift uncertainty is also specified as the maximum range of H_2O gain drift for the analyzers (d_{wg}) that varies with ambient air temperature (Campbell Scientific Inc., 2018b), but normally within the specified range as (see Table 1):

$$d_{wg} = \pm\delta_{H_2O\_g}\chi_{H_2O\_T} \tag{16}$$

where $\delta_{H_2O\_g}$ is H_2O gain drift percentage and $\chi_{H_2O\_T}$ is the true H_2O mixing ratio. This specification is the maximum range of H_2O measurement uncertainty due to the H_2O gain drift.

The analyzer performs best, almost without gain drift, when T_g is equal to the calibration/span ambient air temperature (T_c, the reason why T_c still is used here is that zero and span procedures should be performed under similar ambient air temperature conditions). The further T_g is away from T_c the more likely it drifts. Using the same way to formulate H_2O zero drift uncertainty, H_2O gain drift uncertainty can be approximated for its maximum range as:

$$\Delta\chi^{g}_{H_2O} = \pm\delta_{H_2O\_g}\chi_{H_2O\_T} \times \begin{cases} \dfrac{T_g - T_c}{T_{rh} - T_{rl}} & T_c < T_g < T_{rh} \\ \dfrac{T_c - T_g}{T_{rh} - T_{rl}} & T_c > T_g > T_{rl} \end{cases} \tag{17}$$

Given the measured value of H_2O mixing ratio is represented by χ_{H_2O}, according to Equation 6, the difference between true and measured H_2O mixing ratios can be expressed as

$$\chi_{H_2O} - \chi_{H_2O\_T} = \Delta\chi^{z}_{H_2O} + \Delta\chi^{g}_{H_2O} + \Delta\chi^{s}_{H_2O} + \Delta\chi^{p}_{H_2O} \tag{18}$$

From this equation, the true H_2O mixing ratio is given by:

$$\chi_{H_2O\_T} = \chi_{H_2O} - \left(\Delta\chi^{z}_{H_2O} + \Delta\chi^{g}_{H_2O} + \Delta\chi^{s}_{H_2O} + \Delta\chi^{p}_{H_2O}\right) \tag{19}$$

The term inside the round brackets in this equation is an error term, which generally is smaller, at least, one order than the true value in magnitude. Although the case would not be so true for H_2O in cold ecosystems (e.g., <−5°C) and/or dry environments, measured value is an appropriate alternative, with the most likelihood, to the true value for the applications of Equation 17. As such, $\chi_{H_2O\_T}$ in Equation 17 can be reasonably approximated by χ_{H_2O} for equation applications. Using this approximation, Equation 17 becomes:

$$\Delta\chi^{g}_{H_2O} = \pm\delta_{H_2O\_g}\chi_{H_2O} \times \begin{cases} \dfrac{T_g - T_c}{T_{rh} - T_{rl}} & T_c < T_g < T_{rh} \\ \dfrac{T_c - T_g}{T_{rh} - T_{rl}} & T_c > T_g > T_{rl} \end{cases} \tag{20}$$

with χ_{H_2O} from measurements, this equation is applicable in estimation for the H_2O gain drift uncertainty.

4.3. S_c and $\Delta\chi^s_{H_2O}$ (Sensitivity-To-CO_2 Uncertainty)

Since CO_2 is a weak absorber at the infrared wavelength for H_2O measurements (i.e., 2.7 μm, see Figure 4.7 in Wallace & Hobbs, 2006), it can slightly interfere with H_2O absorption at this unique wavelength (McDermitt et al., 1993). As such, the power of the same measurement light through several H_2O gas samples with the same H_2O molar concentration but different backgrounds of CO_2 amounts would be detected with different values of A_w for the working equation (see Model [12]). Without the S_c term in this equation, different A_w values must result in significantly different ρ_{H_2O} values although ρ_{H_2O} is essentially the same. To report the same ρ_{H_2O} for the air flows with the same H_2O molar concentration under different CO_2 backgrounds, the different values of A_w associated with the same ρ_{H_2O} must be accounted for by S_c associated with A_c and A_{cs} in the working equation (see Model [12]). Similar to Z_w and G_w in the equation, S_c can have an uncertainty in determination of χ_{H_2O}. This uncertainty is specified for the gas analyzers by the sensitivity-to-CO_2 (s_c). For EC155 gas analyzers, the sensitivity-to-CO_2 is specified as $\pm 5 \times 10^{-5}$ mmolH_2O mol^{-1} (μmolCO_2 mol^{-1})$^{-1}$ (Table 1). As the gas analyzers should be calibrated to produce the minimal uncertainty due to this sensitivity for H_2O measurements around atmospheric background CO_2 of 415 μmolCO_2 mol^{-1} (Global Monitoring Laboratory, 2021), the uncertainty in χ_{H_2O} measurements due to sensitivity-to-CO_2 ($\Delta\chi^s_{H_2O}$) can be quantified as

$$\Delta\chi^s_{H_2O} \equiv s_c\left(\chi_{CO_2} - 415\right) \quad 0 \le \chi_{CO_2} \le 1000\,\mu\text{mol}CO_2\ \text{mol}^{-1} \tag{21}$$

Under the atmospheric boundary-layer conditions, χ_{CO_2} commonly ranges from 350 to 800 μmolCO_2 mol^{-1} (LI-Cor Biosciences, 2016). Therefore, using Equation 21, $\Delta\chi^s_{H_2O}$ satisfies:

$$\left|\Delta\chi^s_{H_2O}\right| \le 585\left|s_c\right| \tag{22}$$

4.4. $\Delta\chi_{H_2O}$ (H_2O Measurement Accuracy)

Substituting Equations 11, 14, 20 and 22 into Equation 10, $\Delta\chi_{H_2O}$ can be expressed as

$$\Delta\chi_{H_2O} = \pm\left[1.96\sigma_{H_2O} + 585|s_c| + \left(|d_{wz}| + \delta_{H_2O\_g}\chi_{H_2O}\right) \times \begin{cases} \dfrac{T_g - T_c}{T_{rh} - T_{rl}} & T_c < T_g < T_{rh} \\ \dfrac{T_c - T_g}{T_{rh} - T_{rl}} & T_c > T_g > T_{rl} \end{cases}\right] \tag{23}$$

This equation is the H_2O accuracy equation of CPEC systems. It expresses the accuracy of field χ_{H_2O} measurements from CPEC infrared gas analyzers in terms of its specifications: σ_{H_2O}, s_c, d_{wz}, and $\delta_{H_2O\_g}$; measured variables χ_{H_2O} and T_g; and a known variable T_c. Using this equation and analyzer specification values, the accuracy of field H_2O measurements can be evaluated as a range.

4.5. Evaluation on $\Delta\chi_{H_2O}$

Given the values of T_g, T_c, and χ_{H_2O} and the analyzer specification values of σ_{H_2O}, s_c, d_{wz}, and $\delta_{H_2O\_g}$, the accuracy of χ_{H_2O} measurements can be evaluated over a domain of T_g and χ_{H_2O}. To visualize the relationship of accuracy with T_g and χ_{H_2O}, the accuracy is a dependent (the ordinate) of T_g (the abscissa) at different levels of χ_{H_2O}. In addition, this relationship should be evaluated within possible ranges of T_g and χ_{H_2O} that are typically observed in ecosystems.

In practice, T_g can be approximated with ambient air temperature (T_a) in a range of CPEC operations from −30 to 50°C. To evaluate the accuracy under a standard condition instead of a specific field site, T_c can be set at 20°C, along with atmospheric pressure at 101.325 kPa, as Normal Temperature and Pressure (Wright et al., 2003).

H_2O mixing ratio can be measured by the analyzers from 0 to 79 mmolH_2O mol^{-1}. However, due to the positive dependence of air water vapor saturation on T_a (Wallace & Hobbs, 2006), χ_{H_2O} has a range wider at higher T_a and narrower at lower T_a. At T_a below 40°C under the atmospheric pressure of 101.325 kPa (Wright et al., 2003), χ_{H_2O} is lower than 79 mmolH_2O mol^{-1} and, as T_a decreases, its range becomes narrower and

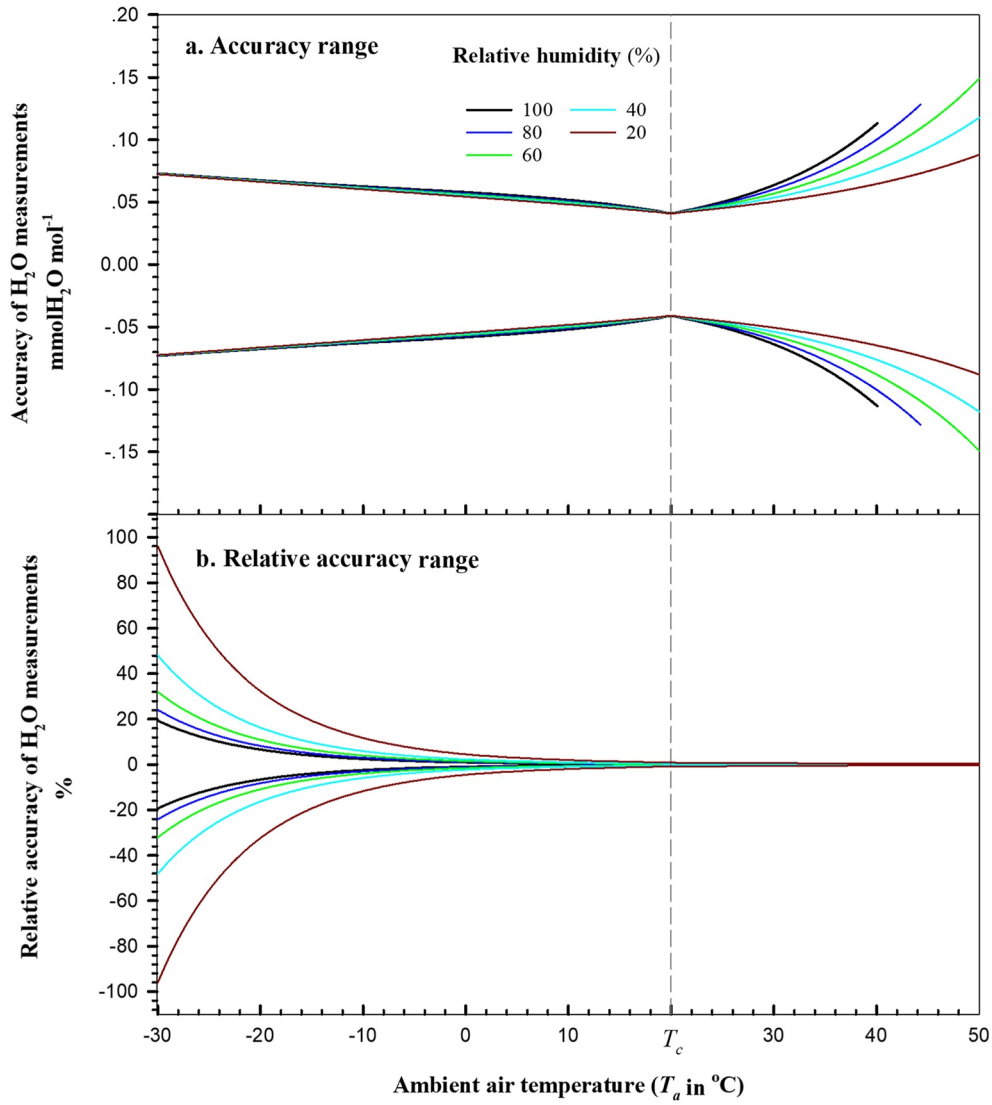

Figure 2. Accuracy of field H_2O measurements from EC155 infrared gas analyzers in closed-path eddy-covariance (CPEC) systems (Campbell Scientific Inc., UT, US) over the operational range of CPEC systems in ambient air temperature from −30 to 50°C under the atmospheric pressure of 101.325 kPa. The vertical dashed line represents ambient air temperature, T_c, at which the analyzers were calibrated, zeroed, and/or spanned. a. Accuracy of H_2O mixing ratio measurements and b. Relative accuracy of H_2O mixing ratio measurements (i.e., the ratio of accuracy to H_2O mixing ratio).

narrower to be 0 to 0.38 $mmolH_2O\ mol^{-1}$ at −30°C. To present the accuracy over the same relative range of air moisture even at different T_a, the saturation water vapor pressure is used to scale air moisture to 20%, 40%, 60%, 80%, and 100% (i.e., relative humidity [RH]). For each scaled RH value, χ_{H_2O} can be calculated at different T_a and P (Appendix A) for the curves of H_2O accuracy equation with equal RH in Figure 2a.

At $T_a = T_c$, the χ_{H_2O} accuracy is the best at its narrowest range and its magnitude is equal to the sum of precision and sensitivity-to-CO_2 uncertainties (<0.0410 $mmolH_2O\ mol^{-1}$ in magnitude). However, away from T_c, its non-linear range becomes wider, gradually below this T_c value but more abruptly above, because, as T_a increases, χ_{H_2O} at the same RH increases exponentially (Equations A1 and A3 in Appendix A) while $\Delta\chi_{H_2O}$ increases linearly with χ_{H_2O} in the H_2O accuracy Equation 23. For a case of T_c at 20°C, the range can be summarized as widest to be ±0.11 $mmolH_2O\ mol^{-1}$ below 40°C and to be ±0.15 $mmolH_2O\ mol^{-1}$ above (Figure 2a and H_2O columns in Table 2). In reference to this wider range (±0.15 $mmolH_2O\ mol^{-1}$), the poorest overall accuracy of H_2O measurements from our study systems can be specified as ±0.15 $mmolH_2O\ mol^{-1}$.

Table 2
Accuracy of CO_2/H_2O Measurements From EC155 Infrared Gas Analyzers in Closed-Path Eddy-Covariance Systems (Campbell Scientific Inc., UT, US) on the Major Values of Background in Ambient Air Temperature, CO_2, and H_2O in Ecosystems (Atmospheric Pressure: 101.325 kPa. Calibration Ambient Air Temperature: 20°C)

	CO_2				H_2O			
	415 μmolCO_2 mol^{-1}		1,000 μmolCO_2 mol^{-1}		60% relative humidity		Saturated	
	Accuracy±	Relative accuracy±	Accuracy±	Relative accuracy±	Accuracy±	Relative accuracy±	Accuracy±	Relative accuracy±
Ambient air temperature °C	μmolCO_2 mol^{-1}	%	μmolCO_2 mol^{-1}	%	mmolH_2O mol^{-1}	%	mmolH_2O mol^{-1}	%
−30	0.7409	0.18	N/A[a]		0.0727	32.12	0.0730	19.34
−25	0.6962	0.17			0.0698	18.52	0.0702	11.18
−22	0.6694	0.16			0.0681	13.44	0.0686	8.12
−20	0.6515	0.16			0.0669	10.89	0.0675	6.59
−18	0.6336	0.15			0.0658	8.85	0.0665	5.36
−15	0.6068	0.15			0.0642	6.52	0.0650	3.96
−10	0.5621	0.14			0.0615	3.97	0.0627	2.43
−6	0.5264	0.13			0.0594	2.70	0.0608	1.66
−5	0.5174	0.12			0.0589	2.46	0.0604	1.51
−2	0.4906	0.12			0.0573	1.85	0.0590	1.14
0	0.4728	0.11			0.0562	1.54	0.0581	0.95
2	0.4549	0.11			0.0551	1.31	0.0570	0.81
5	0.4281	0.10	0.5378	0.05	0.0533	1.02	0.0553	0.63
6	0.4191	0.10	0.5215	0.05	0.0527	0.94	0.0547	0.58
10	0.3834	0.09	0.4565	0.05	0.0500	0.68	0.0519	0.42
15	0.3387	0.08	0.3753	0.04	0.0461	0.45	0.0474	0.28
18	0.3119	0.08	0.3265	0.03	0.0432	0.35	0.0438	0.21
20	0.2940	0.07	0.2940	0.03	0.0410	0.29	0.0410	0.17
22	0.3119	0.08	0.3265	0.03	0.0435	0.27	0.0443	0.16
25	0.3387	0.08	0.3753	0.04	0.0477	0.25	0.0502	0.16
30	0.3834	0.09	0.4565	0.05	0.0569	0.22	0.0637	0.15
35	0.4281	0.10	0.5378	0.05	0.0698	0.20	0.0835	0.14
38	0.4549	0.11	0.5865	0.06	0.0799	0.20	0.0996	0.14
40	0.4728	0.11	0.6190	0.06	0.0879	0.19	0.1126	0.14
42	0.4906	0.12	0.6515	0.07	0.0970	0.19	N/A[b]	
45	0.5174	0.12	0.7003	0.07	0.1133	0.19		
50	0.5621	0.14	0.7815	0.08	0.1489	0.19		

[a]CO_2 mixing ratio is assumed to be lower than 1,000 μmolCO_2 mol^{-1} in ambient air temperature below 5°C in ecosystems. [b]H_2O mixing ratio in saturated air above 40°C under atmospheric pressure of 101.325 kPa is out of the EC155 measurement range (0–79 mmolH_2O mol^{-1}).

Figure 2b shows a pattern of relative accuracy of H_2O measurements with T_a. Given a RH above 20%, the relative accuracy diverges to almost 100% as T_a decreases down to −30°C and converges to 0.35% as T_a increases up to 50 °C. Given the magnitude of accuracy is in a small order (i.e., <0.15 mmolH_2O mol^{-1}), the divergent pattern is shaped by the exponential decrease in χ_{H_2O} saturation amount as T_a decreases and the convergent pattern is shaped by the exponential increase in χ_{H_2O} stauration amount as T_a increases (see Appendix A). At any T_a value, the relative accuracy range also can be wide if RH is near zero (i.e., very dry conditions). In ecosystems, unlike CO_2, H_2O naturally varies "relatively" large across three orders more in a magnitude

(e.g., from 0.04 mmolH_2O mol^{-1}, when RH is 10% at −30°C under the atmospheric pressure of 101.325 kPa, to 59 mmolH_2O mol^{-1}, when dew point temperature is 35°C under the same atmospheric pressure [National Weather Service, 2021]). Under cold and/or dry conditions, the minimum H_2O amount could be several orders smaller than the measurement precision of the gas analyzers. In this case, the relative accuracy would be very large and, without specifying the H_2O status on the measurement background, would not be an appropriate measure to specify the uncertainty of H_2O measurements from gas analyzers. Accordingly, an unconditional specification of relative accuracy for H_2O measurements from infrared gas analyzers would mislead users.

To narrow both accuracy and relative accuracy ranges for H_2O measurements in a lower range of T_a or χ_{H_2O}, frequent zero procedures are needed. Both ranges in Figure 2 are first separately maximized by this study from all uncertainty sources, which is a more solid base for error analysis in H_2O data applications.

5. Accuracy of CO_2 Mixing Ratio Measurements

Accuracy model (9) defines the accuracy of field CO_2 measurements from gas analyzers ($\Delta\chi_{CO_2}$) as

$$\Delta\chi_{CO_2} \equiv \pm\left(\left|\Delta\chi^z_{CO_2}\right| + \left|\Delta\chi^g_{CO_2}\right| + \left|\Delta\chi^s_{CO_2}\right| + \left|\Delta\chi^p_{CO_2}\right|\right) \tag{24}$$

where $\Delta\chi^z_{CO_2}$is CO_2 zero drift uncertainty, $\Delta\chi^g_{CO_2}$is CO_2 gain drift uncertainty, $\Delta\chi^s_{CO_2}$ is sensitivity-to-H_2O uncertainty, and $\Delta\chi^p_{CO_2}$ is CO_2 precision uncertainty.

5.1. $\Delta\chi^p_{CO_2}$(CO_2 Precision Uncertainty)

Using the same approach for $\Delta\chi^p_{H_2O}$, $\Delta\chi^p_{CO_2}$ is formulated as:

$$\Delta\chi^p_{CO_2} = \pm 1.96 \times \sigma_{CO_2} \tag{25}$$

5.2. $\Delta\chi^z_{CO_2}$(CO_2 Zero Drift Uncertainty) and $\Delta\chi^g_{CO_2}$(CO_2 Gain Drift Uncertainty)

The working model of gas analyzers for χ_{CO_2} is similar to Model (12) for χ_{H_2O} in formulation, according to LI-Cor Biosciences (2016), given by:

$$\begin{aligned}\rho_{CO_2} &= P\sum_{i=1}^{5} a_{ci}\left\{1-\left[\frac{A_c}{A_{cs}} + S_w\left(1-\frac{A_w}{A_{ws}}\right)\right]Z_c\right\}^i\left\{\frac{G_c}{P}\right\}^i \\ \chi_{CO_2} &= \rho_{CO_2}\left[\frac{P}{R^*\left(T_g+273.15\right)} - \frac{\rho_{H_2O}}{1000}\right]^{-1}\end{aligned} \tag{26}$$

where ρ_{CO_2} is CO_2 molar concentration (μmolCO_2 m^{-3}); a_{ci} (i = 1, 2, 3, 4, or 5) is a coefficient of the fifth order polynomial in the terms inside curly brackets; S_w is the cross-sensitivity of the detector to H_2O, while detecting CO_2, in the wavelength for CO_2 measurements (hereinafter referred as sensitivity-to-H_2O); Z_c is CO_2 zero adjustment (i.e., CO_2 zero coefficient); G_c is CO_2 gain adjustment (i.e., CO_2 gain coefficient commonly as CO_2 span coefficient). The parameters of a_{ci}, Z_c, G_c, and S_w in this model are statistically estimated to establish a CO_2 working equation in the production calibration against a series of standard CO_2 gases over the ranges of ρ_{H_2O} and P (hereinafter referred as calibration). The CO_2 working equation (i.e., Model [26] with estimated parameters) is used inside the gas analyzer to compute ρ_{co_2} and χ_{co_2} from field measurements of A_c, A_{cs}, A_w, A_{ws}, P, and T_g.

Because of similarity in model principals and parameter implications between Models (12) and (26), using the same analyses and rationales as for$\Delta\chi^z_{H_2O}$ and $\Delta\chi^g_{H_2O}$, $\Delta\chi^z_{CO_2}$ is formulated as:

$$\Delta\chi^z_{CO_2} \equiv d_{cz} \times \begin{cases} \dfrac{T_g - T_c}{T_{rh} - T_{rl}} & T_c < T_g < T_{rh} \\ \dfrac{T_c - T_g}{T_{rh} - T_{rl}} & T_c > T_g > T_{rl} \end{cases} \tag{27}$$

where d_{cz} is the maximum CO_2 zero drift specified for gas analyzers, and $\Delta\chi^{g}_{CO_2}$ is formulated as:

$$\Delta\chi^{g}_{CO_2} \equiv \pm\delta_{CO_2\_g}\chi_{CO_2} \times \begin{cases} \dfrac{T_g - T_c}{T_{rh} - T_{rl}} & T_c < T_g < T_{rh} \\ \dfrac{T_c - T_g}{T_{rh} - T_{rl}} & T_c > T_g > T_{rl} \end{cases} \tag{28}$$

where $\delta_{co_2\_g}$ is the maximum CO_2 gain drift percentage specified for gas analyzers. Both d_{cz} and $\delta_{CO_2\_g}$ are given in analyzer specifications (Table 1).

5.3. $\Delta\chi^{s}_{CO_2}$ (CO_2 Sensitivity-To-H_2O Uncertainty)

Since H_2O also is a weak absorber at the infrared wavelength for CO_2 measurements (i.e., 4.3 μm, Campbell Scientific Inc., 2018a; LI-COR Biosciences 2016), it interferes with CO_2 absorption slightly (McDermitt et al., 1993). As such, the power of identical measurement light through several gas samples with the same CO_2 molar concentration but different backgrounds of H_2O molar concentrations would result in different values of A_c into the CO_2 working equation. Without the S_w term in this equation, different A_c values will result in significantly different ρ_{CO_2} values although ρ_{CO_2} is actually the same. To report the same ρ_{CO_2} for the air flows with the same CO_2 molar concentration under different H_2O backgrounds, the different values of A_c associated with ρ_{CO_2} must be accounted for by S_w associated with A_w and A_{ws} as shown in Model (26). However, S_w can have an uncertainty in its accountability. This uncertainty is specified by the sensitivity-to-H_2O (s_w). For EC155 gas analyzers, the sensitivity-to-H_2O is specified as $\pm 5.6 \times 10^{-8}$ $\mu molCO_2\ mol^{-1}$ $(mmolH_2O\ mol^{-1})^{-1}$ (Table 1). Given that the gas analyzers for CO_2 works best for dry air, the uncertainty in χ_{co_2} measurements due to sensitivity-to-H_2O ($\Delta\chi^{s}_{CO_2}$) can be quantified as

$$\Delta\chi^{s}_{CO_2} \equiv s_w\chi_{H_2O} \quad 0 \le \chi_{H_2O} \le 79\,mmolH_2O\ mol^{-1} \tag{29}$$

Accordingly, $\Delta\chi^{s}_{CO_2}$ can be reasonably expressed as:

$$\left|\Delta\chi^{s}_{CO_2}\right| \le 79\left|s_w\right| \tag{30}$$

5.4. $\Delta\chi_{CO_2}$ (CO_2 Measurement Accuracy)

Substituting Equations 25, 27, 28 and 30 into Equation 24, $\Delta\chi_{CO_2}$ can be expressed as:

$$\Delta\chi_{CO_2} = \pm\left[1.96\sigma_{CO_2} + 79\left|s_w\right| + \left(\left|d_{cz}\right| + \delta_{CO_2\_g}\chi_{CO_2}\right) \times \begin{cases} \dfrac{T_g - T_c}{T_{rh} - T_{rl}} & T_c < T_g < T_{rh} \\ \dfrac{T_c - T_g}{T_{rh} - T_{rl}} & T_c > T_g > T_{rl} \end{cases}\right] \tag{31}$$

This equation is the CO_2 accuracy equation of infrared gas analyzers in CPEC systems. It expresses the accuracy of χ_{CO_2} measurements from the analyzers in terms of their specifications: σ_{CO_2}, s_w, d_{cz}, and $\delta_{co_2\_g}$; measured variables χ_{CO_2} and T_g; and a known variable T_c. Using this equation and analyzer specification values, the accuracy of field CO_2 measurements can be evaluated as a range.

5.5. Evaluation on $\Delta\chi_{CO_2}$

Using the CO_2 accuracy Equation 31 along with the analyzer specifications of σ_{CO_2}, s_w, d_{cz}, and $\delta_{co_2\_g}$, $\Delta\chi_{CO_2}$ can be evaluated over a domain of T_g and χ_{CO_2} for a given T_c. Similar to the presentation of H_2O accuracy in Figure 2, $\Delta\chi_{CO_2}$ is a dependent (the ordinate) of T_g (the abscissa) from −30 to 50°C at different levels of χ_{co_2} within the range typically observed in ecosystems. T_c is set for the normal temperature of 20°C (Wright et al., 2003) and T_g is surrogated by T_a (Figure 3).

5.5.1. χ_{CO_2} Range

χ_{CO_2} is measured by the EC155 infrared CO_2/H_2O analyzers up to 1,000 $\mu molCO_2\ mol^{-1}$. In the atmosphere, χ_{CO_2} average is currently ~415 $\mu molCO_2\ mol^{-1}$ (Global Monitoring Laboratory, 2021). However, in

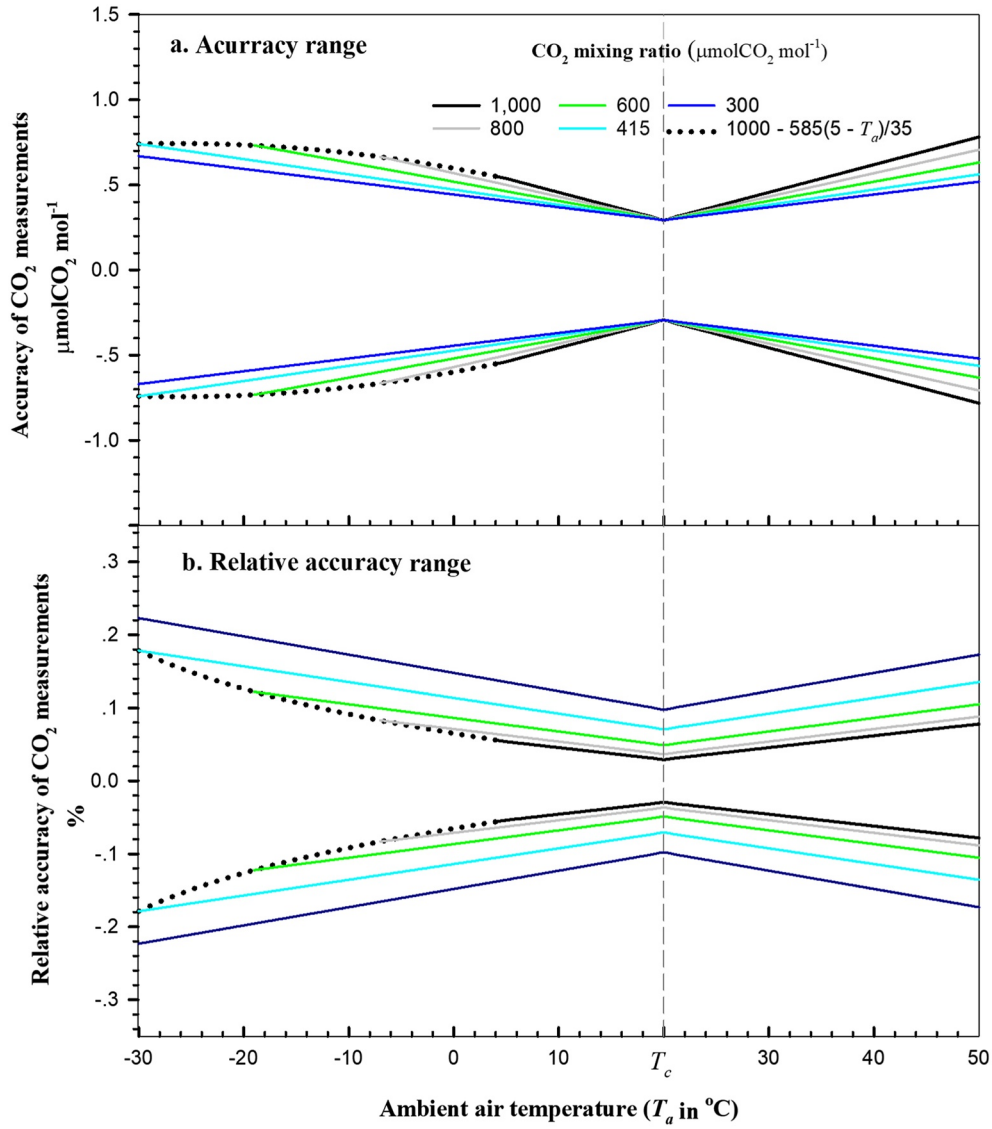

Figure 3. Accuracy of field CO_2 measurements from the EC155 infrared gas analyzers in closed-path eddy-covariance systems over the operational ranges of ambient air temperature (−30° to 50°C) at 101.325 kPa atmospheric pressure. The vertical dashed line represents ambient air temperature, T_c, at which an analyzer was calibrated, zeroed, and/or spanned. When T_a decreases from 5° to −30°C, CO_2 mixing ratio on black dotted lines linearly decreases from 1,000 μmolCO_2 mol^{-1} at 5°C to 415 μmolCO_2 mol^{-1} (i.e., atmospheric background value) at −30°C. (a) Accuracy of CO_2 mixing ratio measurements and (b) Relative accuracy of CO_2 mixing ratio measurements (i.e., the ratio of accuracy to CO_2 mixing ratio).

terrestrial ecosystems, where the analyzers are deployed, χ_{CO_2} fluctuates with human induced emissions and biological processes such as plant physiological metabolism, soil microganism respiration, and animal physiological activities (Wang et al., 2016); aerodynamic regimes such as wind speed, wind direction related to terrain topography (de Araújo et al., 2010), and vertical wind gradient (Yang et al., 2007); and thermodynamic states such as air temperature, soil temperature, and boundary-layer stability (Ohkubo et al., 2008). As discussed above, χ_{CO_2} in ecosystems commonly ranges from 350 to 800 μmolCO_2 mol^{-1} depending on biological processes, aerodynamic regimes, and thermodynamic states. This range is extended from 300 to 1,000 μmolCO_2 mol^{-1} as the possible range within which $\Delta\chi_{CO_2}$ is evaluated. Because of the dependence of $\Delta\chi_{CO_2}$ on χ_{CO_2} (Equations 28 and 31), to show the accuracy at different levels of χ_{CO_2}, the range is further divided into five grades of 300, 415 (atmospheric background value), 600, 800, and 1000 μmolCO_2 mol^{-1} for evaluation presentations as in Figure 3a.

However, in terrestrial ecosystems, with decreasing T_a from its plant physiological threshold for growth and development, biological processes diminish. Generally, while T_a decreases from 5°C to negative, plants and microorganisms gradually go dormant or finish their life spans if frozen (Taiz et al., 2014). In such a process, however, soil temperature related to microorganism respiration and/or activities in deeper layers decreases in lag (Widén & Majdi, 2001). While T_a is below 0°C, soil temperature at some depths is likely still above freezing, and soil microorganisms are still active (Rosenberg et al., 1983). Due to the activities sometimes under the conditions of low wind along with atmospheric stable stratification, χ_{CO_2} in ecosystems may still be higher than the CO_2 background concentration (Nicolini et al., 2018), but it should approach this background concentration at very low T_a. The value of −30°C at the low end of the specified temperature range for CPEC operations can be considered lower than enough. While T_a decreases to −30°C, the χ_{CO_2} in ecosystems, if higher, should gradually decrease to the CO_2 background value. Accordingly, χ_{CO_2}, if higher, should start at 5°C to converge asymptotically to 415 $\mu molCO_2\ mol^{-1}$ at −30°C. Without the asymptotical function for the convergence boundary of curve trend, the convergence can be conservatively assumed as a simple linear trend from 1,000 (i.e., maximum) to 415 $\mu molCO_2\ mol^{-1}$ as the boundary while T_a decreases from 5° to −30°C. The CO_2 measurement accuracy, $\Delta\chi_{CO_2}$, at each CO_2 grade is evaluated up to the boundary on the dotted trend curve as shown in Figure 3.

5.5.2. $\Delta\chi_{CO_2}$ Evaluation

At $T_a = T_c$, the χ_{CO_2} accuracy is the best at its narrowest range and its magnitude is the sum of precision and sensitivity-to-H_2O uncertainties (0.29 $\mu molCO_2\ mol^{-1}$). However, away from T_c, its range expands in a near-linear fashion. In case of T_c at 20°C, the $\Delta\chi_{CO_2}$ range can be summarized as a maximum to be $\pm 0.78\ \mu molCO_2\ mol^{-1}$ in ecosystems at the extreme conditions (e.g., 50°C. Figure 3a and CO_2 columns in Table 2). The relative CO_2 accuracy has its maximum range of ±0.23% (Figure 3b).

Same as Figure 2, both ranges in Figures 3a and 3b are first separately maximized by this study from all uncertainty sources, which is a more solid base for error analyses in CO_2 data applications.

6. Discussion

The primary objective of this study is to quantify the accuracy of field CO_2/H_2O measurements by infrared gas analyzers in CPEC systems from their specifications for their zero drift, gain drift, sensitivity-to-CO_2/H_2O, and precision. In practice, the accuracy is used to quantify the uncertainty of CO_2/H_2O data for applications. Additionally, the relationship of accuracy to different specification terms (e.g., gain drift) as component uncertainties can be considered as rationale to guide the analyzer field maintenance in maximally improving field measurement accuracy.

6.1. Application Example

As discussed in the introduction, χ_{H_2O}along with T_s is applicable to calculate T_a (Kaimal & Gaynor, 1991). Given the function, $T_a\left(\chi_{H_2O}, T_s\right)$, from a theoretical basis of first principles, the equation itself does not have any error and the calculated T_a should be accurate as long as the values of χ_{H_2O} and T_s are exact. For our subject, however, χ_{H_2O} and T_s are measured by the CPEC systems deployed in the field under changing environments. Their measured values must include measurement uncertainty in χ_{H_2O}, denoted by $\Delta\chi_{H_2O}$ (i.e., field χ_{H_2O} measurement accuracy), and in T_s as well, denoted by ΔT_s (i.e., field T_s measurement accuracy). $\Delta\chi_{H_2O}$ and/or ΔT_s unavoidably propagate to the calculated T_a through equation output as uncertainty, denoted by ΔT_a. In numerical analysis (Burden & Faires, 1993) or in statistics (Snedecor & Cochran, 1989), any applicable equation requires the specification for its uncertainty term. Therefore, $T_a\left(\chi_{H_2O}, T_s\right)$ should include a specification of the respective accuracy expressed as uncertainty bounds, which are the maximum and minimum limits of calculated T_a for any given pair of $\chi_{H_2O}$and T_s. This accuracy is needed by any application. It should be specified through the relationship of ΔT_a to $\Delta\chi_{H_2O}$ and ΔT_s.

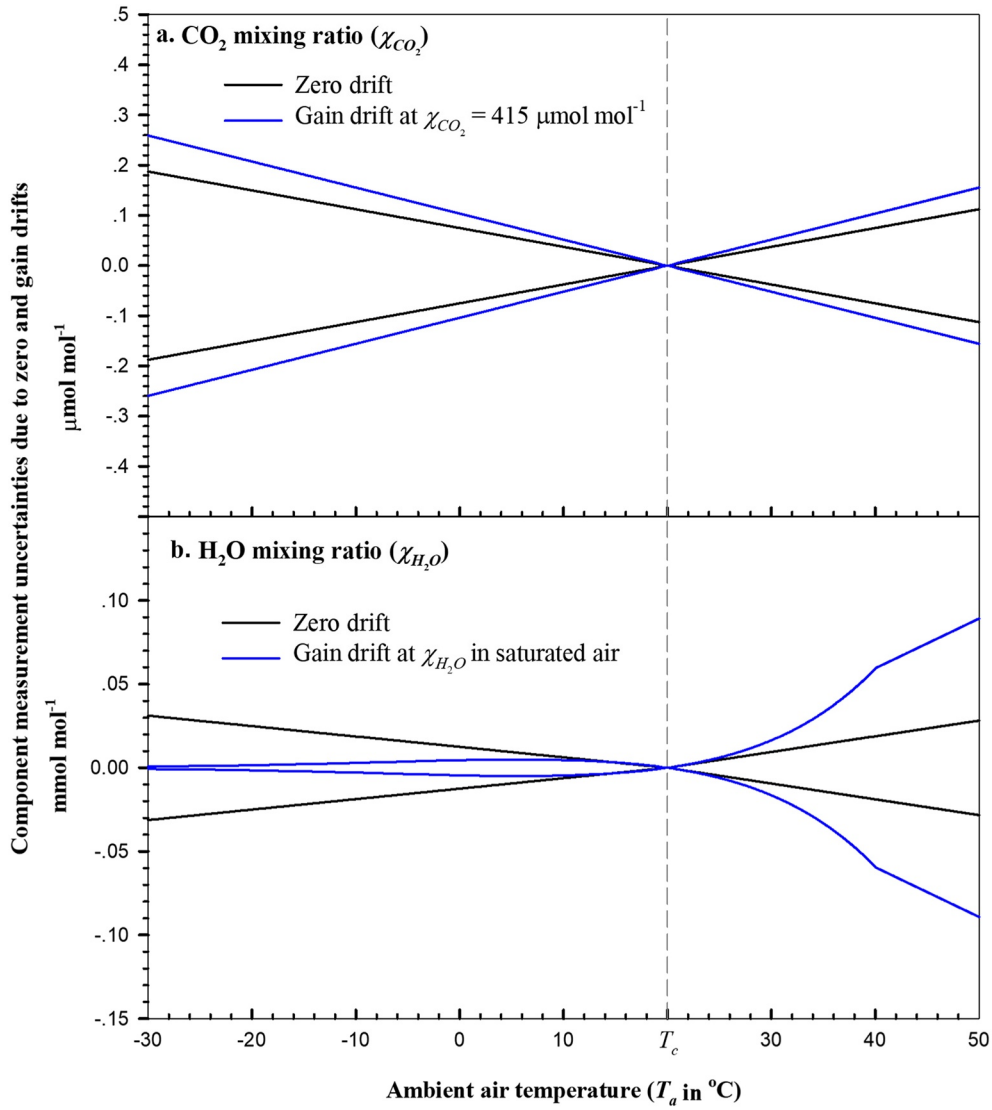

Figure 4. Component measurement uncertainties due to the zero and gain drifts of EC155 infrared gas analyzers in closed-path eddy-covariance systems over the operational range of ambient air temperature under the atmospheric pressure of 101.325 kPa. (a) Zero and gain drift uncertainties in χ_{co_2} measurements and (b) Zero and gain drift uncertainties in χ_{H_2O} measurements. Dashed line represents ambient air temperature, T_c, at which an analyzer was calibrated, zeroed, and/or spanned.

As field measurement accuracies, both $\Delta\chi_{H_2O}$ and ΔT_s can be reasonably considered as small increments in a calculus sense. Following the principles of differential equation and considering that χ_{H_2O} and T_s are measured from two independent sensors, ΔT_a is a total differential of $T_a\left(\chi_{H_2O}, T_s\right)$ with respect to χ_{H_2O} and T_s, given by:

$$\Delta T_a = \frac{\partial T_a\left(\chi_{H_2O}, T_s\right)}{\partial \chi_{H_2O}} \Delta\chi_{H_2O} + \frac{\partial T_a\left(\chi_{H_2O}, T_s\right)}{\partial T_s} \Delta T_s \tag{32}$$

Apparently, $\Delta\chi_{H_2O}$ is a required term for evaluation of ΔT_a. In this equation, the two partial derivatives can be derived from the explicit function of $T_a\left(\chi_{H_2O}, T_s\right)$, $\Delta\chi_{H_2O}$ is estimated by the application of this study, and ΔT_s can be acquired from the specification for 3D sonic anemometers (Zhou et al., 2018). With the two partial derivatives, $\Delta\chi_{H_2O}$, and ΔT_s, ΔT_a can be evaluated as a function of χ_{H_2O} and T_s.

6.2. Rationale to Guide Analyzer Field Maintenance

An infrared gas analyzer works at its best in the same environment as its manufacturing conditions, which is shown in Figures 2 and 3 for measurement accuracies associated with T_c. The analyzer works better while T_a is closer to T_c. However, in practice, it is deployed commonly for long-term measurements in the field under changing weather conditions through seasonal climates. Most of the time these conditions are different from those in the manufacturing process. Over time, the analyzer gradually drifts to some degree, although the drifts should be within its specifications, and needs maintenance.

As discussed in Sections 4 and 5, the uncertainty in analyzer measurements from the sources of precision and sensitivity-to-CO_2/H_2O uncertainties is not improvable through field maintenance, but it is small ($\pm$0.29 $\mu molCO_2\ mol^{-1}$ for CO_2, Equations 25, 30 and 31, and $\pm$0.04 $mmolH_2O\ mol^{-1}$ for H_2O, Equations 11, 22 and 23). However, the zero and gain drifts of analyzers are major components of uncertainty in determination of their field measurement accuracies (Figures 2–4, Equations 14, 20, 27 and 28). Fortunately, the drifts are adjustable through the zero and span procedures (see Sections 4.1 and 4.2). The procedures are recommended to minimize the drift influence on field measurement uncertainties. Therefore, the manufacturers of infrared gas analyzers designed software and hardware tools for the procedures and recommended the procedure schedule using the tools (Campbell Scientific Inc., 2018a; LI-COR Biosciences, 2016). As shown in Figures 2–4, this study helps users understand, through visualization, how to schedule, perform, and assess the procedures.

6.2.1. CO_2 Zero and Span Procedures

As shown in Figures 3 and 4a, the CO_2 zero drift and/or CO_2 gain drift can bring appreciable uncertainties to field CO_2 measurements in a similar trend over the full T_a range within which CPEC systems operate. Both drifts should be adjusted near T_a around which a corresponding analyzer runs. Fortunately, unlike the H_2O gas, CO_2 gas can be conveniently used under any T_a environment. Referring to Figure 4a, the zero and gain drifts for field CO_2 measurements should be adjusted, through the zero and span procedures, at T_c close to the daily mean of T_a. A CPEC310 system automatically zeroes and spans its analyzer for field CO_2 measurements in a timing interval set by a user at a resolution of a minute (Campbell Scientific Inc., 2018b). According to the range of T_a daily cycle, the procedures are set around its daily mean. Given that T_a fluctuates within a daily range much narrower than 40°C, the CPEC system can run at T_a within $\pm$20 of T_c. In this way after the procedures, for the case in atmospheric background of CO_2 (i.e., 415 $\mu molCO_2\ mol^{-1}$), the widest possible range of $\pm$0.74 $\mu molCO_2\ mol^{-1}$ (see the left CO_2 accuracy column in Table 2) for field CO_2 measurement accuracy can be narrowed by 36% to $\pm$0.47 $\mu molCO_2\ mol^{-1}$ (estimated according to the CO_2 accuracy at T_a of 20°C above and below calibration ambient air temperature), which would be significant improvement in CO_2 measurements from CPEC automatic CO_2 zero and span procedures.

Additionally, in ecosystems during the growing season, the gain drift likely causes more uncertainty than zero drift due to more events of higher CO_2 mixing ratio from active respiration of soil-plant continuum under stable atmospheric stratification (Widén & Majdi., 2001; Yang et al., 2007). In such a season, more frequent CO_2 span procedures are preferred as if a CPEC310 system (Campbell Scientific Inc., UT, US) ran with automatic zero and CO_2 span procedures at a timing interval optionally set by a user.

6.2.2. H_2O Zero and Span Procedures

As shown in Figure 4b, the uncertainty in H_2O measurements from the zero drift increases with T_a away from T_c in the same way as for CO_2 measurements. Therefore, H_2O zero procedure should be performed in the same way as for CO_2 zero procedure. However, the uncertainty from the gain drift exponentially diverges, as T_a increases away from T_c, up to $\pm$0.0892 $mmolH_2O\ mol^{-1}$ at 50°C (from data for Figure 4b) and gradually converges, as T_a decreases away from T_c, down to a small magnitude, $\pm$0.0007 $mmolH_2O\ mol^{-1}$, at $-$30°C (from data for Figure 4b). The exponential divergence above T_c is formed by the exponential increase in air H_2O saturation with T_a increase (Buck, 1981) while the H_2O gain drift uncertainty linearly increases with χ_{H_2O} as T_a increases away from T_c (Equation 20). Below T_c, the gradual convergence is formed by the exponential decrease in air H_2O saturation with T_a decrease although the H_2O gain drift uncertainty still linearly increases with χ_{H_2O} as T_a decreases away from T_c (Equation 20). This trend of H_2O gain drift uncer-

tainty with T_a is a rationale to judge the need of the H_2O span procedure under different environments to adjust the H_2O gain drift.

Given T_c at 20°C (i.e., the H_2O span procedure is performed at 20°C), the uncertainty from gain drift for saturated air at T_a below 0°C is estimated within ±0.0046 mmolH_2O mol^{-1} (from data for Figure 4b). Given T_c equal to 5°C, this estimated uncertainty would be within ±0.0012 mmolH_2O mol^{-1} equal to 5% H_2O zero drift uncertainty, ±0.0219 mmolH_2O mol^{-1}, if not zeroed at T_a below 5°C. In the range of T_a below 0°C, considering the small H_2O gain drift uncertainty and inconvenient application of H_2O span gas from any dew point generator (LI-COR Biosciences, 2004), the H_2O span procedure may be unnecessary, but the H_2O zero procedure becomes critically necessary in narrowing H_2O measurement accuracy. This recommendation eases the users who are worried about H_2O measurement accuracy in the cold seasons during which the H_2O span procedure for analyzers is hardly performed in a convenient way while the H_2O zero procedure still can be automatically performed (Campbell Scientific Inc. 2018a). In contrast, in the higher T_a range (e.g., 30°C, see Figure 2a and Table 2) under humid conditions, this H_2O span procedure must be more frequently needed. Unfortunately, unlike the CO_2 gas, H_2O gas cannot be conveniently used for automatic H_2O span procedure under any T_a environment (LI-COR Biosciences, 2004). Nonetheless, the results from this study emphasize the need for the H_2O span procedure for the gas analyzers at a higher T_a range in humid conditions.

Given that the H_2O and CO_2 zero drifts are automatically adjusted together through all-zero procedure and the H_2O gain drift is manually adjusted through the H_2O span procedure in a manual-recommended interval (Campbell Scientific Inc., 2018a; LI-COR Biosciences, 2016) practically over a range of T_a from 5° to 30°C, the widest range, ±0.15 mmolH_2O mol^{-1}, of H_2O measurement accuracy in case of T_c at 20°C (see the H_2O accuracy column for 60% relative humidity in Table 2) can be narrowed by 27% to ±0.11 mmolH_2O mol^{-1} (estimated by setting T_c as 30°C). While warranting H_2O measurement accuracy, CPEC automatic zero procedure over the system operational range of T_a and the manual H_2O span over a practical range of T_a also can improve the accuracy as analyzed from Figure 2 and Table 2.

6.3. Benefit From the Automatic Zero Procedure

Looking at the saturated H_2O columns in Table 2, the poorest accuracy of H_2O measurements at T_a below 0°C is ±0.073 mmolH_2O mol^{-1}. In the same T_a range, automatically adjusting the zero drift on a daily base for the gas analyzer to run at T_a within ±20°C of T_c, the zero procedure narrows this range by 36% at least to ±0.047 mmolH_2O mol^{-1} (estimated by setting T_c to be −10°C). At the same time, the range of relative accuracy (Figure 2b) can be narrowed by the same percentage. Apparently, while the H_2O span procedure is unnecessary, the accuracy and relative accuracy of H_2O measurements at T_a below 0°C can be greatly benefited from the automatic zero procedure.

7. Concluding Remarks

As advanced by the International Organization for Standardization (2012), measurement accuracy is defined as a combination of trueness (systematic uncertainty) and precision (random uncertainty), being a range of the composite uncertainty from all measurement uncertainty sources. Adopting this definition, the accuracy of field CO_2/H_2O measurements from the infrared gas analyzers in CPEC systems is defined as a maximum range of composite measurement uncertainty sourced from trueness (zero drift, gain drift, and sensitivity-to-CO_2/H_2O uncertainties) and precision (random measurement uncertainty). The analyzers are specified for their measurement performances in terms of zero drift, gain drift, sensitivity-to-CO_2/H_2O, and precision (Campbell Scientific Inc., 2018a). The uncertainty terms are comprehended into accuracy model (10) as a composite uncertainty to describe the accuracy of field CO_2/H_2O measurements from the analyzers. Based on instrumentation technology, the specified uncertainty terms of analyzers calibrated under manufacturer ambient conditions are incorporated into the model. The incorporation formulates CO_2 accuracy Equation 31 and H_2O accuracy Equation 23. According to atmospheric physics and environmental parameters, the equations are used to evaluate the analyzers for their accuracies of field CO_2 and H_2O measurements in ecosystems over the analyzer operational range of ambient air temperature (T_a) under the normal atmospheric pressure of 101.325 kPa (Wright et al., 2003).

The maximum accuracy range of field CO_2 measurements at 415 $\mu molCO_2\ mol^{-1}$ (atmospheric background) from the analyzers is $\pm 0.74\ \mu molCO_2\ mol^{-1}$ (relatively ±0.18%) and at 1,000 $\mu molCO_2\ mol^{-1}$, assumed as the highest CO_2 in ecosystems, is $\pm 0.78\ \mu molCO_2\ mol^{-1}$ (relatively ±0.08%, Figure 3 and Table 2). Accordingly, for the CO_2 measurements in ecosystems from our example gas analyzers, the overall accuracy can be specified as $\pm 0.78\ \mu molCO_2\ mol^{-1}$, relatively being within ±0.18%.

The maximum accuracy range of field H_2O measurements from the gas analyzers can be specified as $\pm 0.15\ mmolH_2O\ mol^{-1}$ (Figure 2a and Table 2). For the H_2O measurements in ecosystems, relative accuracy is not recommended to specify the performance of analyzers, because, without knowing the air moisture level in magnitude for measurements, the relative accuracy in percent for H_2O measurements is not practically descriptive.

Accuracy Equations 23 and 31 are not only applicable for error/uncertainty analyses in CO_2/H_2O data applications (see Section 6.1), but also used as rationales to guide and assess the field maintenances on the gas analyzers. Equation 31, as shown in Figures 3a and 4a, guides users to adjust the CO_2 zero drift through the all-zero (i.e., CO_2/H_2O zero) procedure and the CO_2 gain drift through the CO_2 span procedure. Given that T_a fluctuates within a daily range much narrower than 40 °C, the automatic zero/span procedures could ensure that infrared gas analyzers run at T_a reasonably within ±20 of T_c at which an analyzer is calibrated or zeroed/spanned. As assessed, on the atmospheric CO_2 background, the procedures can narrow the maximum CO_2 accuracy range by 36% from ±0.74 to $\pm 0.47\ \mu molCO_2\ mol^{-1}$.

Equation 23 as shown in Figures 2a and 4b guides users to adjust the H_2O zero drift in the same way as for CO_2. It rationalizes that the H_2O gain drift needs to be adjusted with more attention to the higher T_a range (e.g., above 30°C) under humid conditions. This adjustment is not necessary below 0°C. Given that the H_2O zero drift is automatically adjusted daily through the all-zero procedure, the H_2O gain drift can be manually adjusted through the H_2O span procedure in a manual-recommended interval while T_a is in an operational range of 5°–30°C for H_2O span (i.e., T_c between 5° and 30°C). Such a zero/span protocol could narrow the H_2O accuracy range of ±0.15 by 27% to $\pm 0.11\ mmolH_2O\ mol^{-1}$.

In the T_a range below 0°C, the zero procedure can narrow the H_2O accuracy range of $\pm 0.073\ mmolH_2O\ mol^{-1}$, in case of air saturation, by 36% at least to $\pm 0.047\ mmolH_2O\ mol^{-1}$. At the same time, the range of relative accuracy (Figure 2b) can be narrowed by the same percentage. For cold environments, the unnecessity for H_2O span procedures and greater necessity for automatic all-zero procedures are first addressed in this study. The former relieves users from worrying about the H_2O measurement uncertainty in freezing conditions from the H_2O gain drift, which is not practically adjustable under such conditions. The latter further warrants the accuracy of H_2O along with CO_2 measurements in cold and/or dry environments.

Accuracy model (10), accuracy Equations 23 and 31, and methodology in Sections 4 and 5 use the composite uncertainty of field CO_2/H_2O measurements to define the accuracies for infrared gas analyzers in CPEC systems used in ecosystems. Beyond the applications above, the ultimate objective of this study is to provide an approach for the flux measurement community to specify the accuracy of field CO_2/H_2O measurements in ecosystems from the infrared gas analyzers in CPEC systems and eventually in open-path eddy-covariance systems as well.

Appendix A: Algorithm for Water Vapor Mixing Ratio From Ambient Air Temperature, Relative Humidity, and Atmospheric Pressure

For a given ambient air temperature (T_a in °C) and atmospheric pressure (P in kPa), air has a limited capacity to hold a certain amount of water vapor (Wallace & Hobbs, 2006). This capacity is described in terms of saturation water vapor pressure (e_s in kPa), for moist air, given through the Clausius-Clapeyron equation (Sonntag, 1990):

$$e_s(T_a,P)=\begin{cases}0.6112\exp\left(\dfrac{17.62T_a}{T_a+243.12}\right)f(P) & T_a\geq 0\\ 0.6112\exp\left(\dfrac{22.46T_a}{T_a+272.62}\right)f(P) & T_a<0\end{cases} \tag{A1}$$

where $f(P)$ is an enhancement factor for moist air, being a function of atmospheric pressure: $f(P) = 1.0016 + 3.15 \times 10^{-5} P - 0.0074 P^{-1}$. At relative humidity (RH in %), the water vapor pressure $[e_{\mathrm{RH}}(T_a, P)]$ is:

$$e_{\mathbf{RH}}(T_a, P) = \mathrm{RH} e_s(T_a, P) \tag{A2}$$

Given the mole numbers of H_2O (n_{RH}) and dry air (n_{d}) per unit volume at RH, the water vapor mixing ratio at RH ($\chi^{\mathrm{RH}}_{H_2O}$):

$$\chi^{\mathrm{RH}}_{H_2O} \equiv \frac{n_{\mathbf{RH}}}{n_d} = \frac{n_{\mathbf{RH}} R^*(T_a + 273.15)}{n_d R^*(T_a + 273.15)} = \frac{e_{\mathrm{RH}}(T_a, P)}{P_d} \tag{A3}$$

where R^* is the universal gas constant and P_d is dry air pressure. Using this equation and the relation:

$$P = P_d + e_{\mathrm{RH}}(T_a, P) \tag{A4}$$

$\chi^{\mathrm{RH}}_{H_2O}$ can be expressed in mmolH_2O mol^{-1} as

$$\chi^{\mathrm{RH}}_{H_2O} = \frac{1000 \times e_{\mathrm{RH}}(T_a, P)}{P - e_{\mathrm{RH}}(T_a, P)} \tag{A5}$$

This is used to calculate $\chi^{\mathrm{RH}}_{H_2O}$ in Figures 2 and 4.

Data Availability Statement

The data that support the findings of this study are openly available at https://datadryad.org/stash/share/pdcabKdKQdCo9ug-T-oTRC66Lo4uesR2FCT7hO4inT0.

Acknowledgments
Authors thank Campbell Scientific for providing the images used in Figure 1, anonymous reviewers for their deep insight into this study topic and constructive comments to improve our presentations, and Linda Worlton-Jones for her professional proofreading. This research was supported by the Strategic Priority Research Program of the Chinese Academy of Sciences (XDA19030204), (2016YFC0500300), Long Term Agroecosystem Network (LTAR-USDA), and Campbell Scientific Research and Development.

References

Aubinet, M., Vesala, T., & Papale, D. (Eds). (2012). *Eddy covariance: A practice guide to measurement and data analysis*. New York: Springer.
Buck, A. L. (1981). New equations for computing vapor-pressure and enhancement factor. *Journal of Applied Meteorology*, *20*(12), 1527–1532. https://doi.org/10.1175/1520-0450(1981)020<1527:nefcvp>2.0.co;2
Burden, R. L., & Faires, J. D. (1993). *Numerical analysis* (5th ed.). Boston: PWS Publishing Company.
Campbell Scientific Inc. (2018a). *EC155 CO_2/H_2O closed-path gas analyzer*. (Revision 7/18) (pp. 5–7). Logan, UT.
Campbell Scientific Inc. (2018b). *The CPEC310 advantage*. (Revision 6/14). (p. 1). Logan, UT.
de Araújo, A. C., Dolman, A. J., Waterloo, M. J., Gash, J. H. C., Kruijt, B., Zanchi, F. B., et al. (2010). The spatial variability of CO_2 storage and the interpretation of eddy covariance fluxes in central Amazonia. *Agricultural and Forest Meteorology*, *150*(2), 226–237. https://doi.org/10.1016/j.agrformet.2009.11.005
Fratini, G., McDermitt, D. K., & Papale, D. (2014). Eddy-covariance flux errors due to biases in gas concentration measurements: Origins, quantification and correction. *Biogeosciences*, *11*(4), 1037–1051. https://doi.org/10.5194/bg-11-1037-2014
Global Monitoring Laboratory. (2021). *Trends in atmospheric carbon dioxide*. Retrieved From https://www.esrl.noaa.gov/gmd/ccgg/trends/weekly.html
Ibrom, A., Dellwik, E., Flyvbjerg, H., Jensen, N. O., & Pilegaard, K. (2007). Strong low-pass filtering effects on water vapour flux measurements with closed-path eddy correlation systems. *Agricultural and Forest Meteorology*, *147*(3), 140–156. https://doi.org/10.1016/j.agrformet.2007.07.007
International Organization for Standardization. (2012). *Accuracy (trueness and precision) of measurement methods and results—Part 1: General principles and definitions*.
Joint Committee for Guide in Metrology. (2008). *Evaluation of measurement data: Guide to the expression of uncertainty in measurement* (1st ed.). Research Triangle Park, NC: JCGM Member Organization.
Kaimal, J. C., & Gaynor, J. E. (1991). Another look at sonic thermometry. *Boundary-Layer Meteorology*, *56*(4), 401–410. https://doi.org/10.1007/BF00119215
Leuning, R., & Moncrieff, J. (1990). Eddy-covariance CO_2 flux measurements using open- and closed-path CO_2 analysers: Corrections for analyser water vapour sensitivity and damping of fluctuations in air sampling tubes. *Boundary-Layer Meteorology*, *53*(1), 63–76. https://doi.org/10.1007/BF00122463
LI-COR Biosciences. (2004). *LI-610 Portable dew point generator: Instruction manual* (pp. 3–1~20). Lincoln, NE.
LI-COR Biosciences. (2016). *LI-7500 RS open path CO_2/H_2O gas analyzer: Instruction manual*. (p. 4-1~11–8-1~9). Lincoln, NE.
McDermitt, D. K., Welles, J. M., & Eckles, R. D. (1993). Effects of temperature, pressure and water vapor on gas phase infrared absorption by CO_2. *LI-Cor Application Note*, *116*, 5.
National Weather Service. (2021). *Fast facts*. National Ocean and Atmospheric Administration. Retrieved From https://www.weather.gov
Nicolini, G. M., Aubinet, M., Feigenwinter, C., Heinesch, B., Lindroth, A., Mamadou, O., et al. (2018). Impact of CO_2 storage flux sampling uncertainty on net ecosystem exchange measured by eddy covariance. *Agricultural and Forest Meteorology*, *248*, 228–239. https://doi.org/10.1016/j.agrformet.2017.09.025

Ohkubo, S., Kosugi, Y., Takanashi, S., Matsuo, N., Tani, M., & Nik, A. R. (2008). Vertical profiles and storage fluxes of CO_2, heat and water in a tropical rainforest at Pasoh, Peninsular Malaysia. *Tellus B: Chemical and Physical Meteorology*, *60*(4), 569–582. https://doi.org/10.1111/j.1600-0889.2008.00367.x

Rosenberg, N. J., Blad, B. L., & Verma, S. B. (1983). *Microclimate: The biological environment* (p. 495). New York: John Wiley & Sons.

Schotanus, P., Nieuwstadt, F. T. M., & De Bruin, H. A. R. (1983). Temperature measurement with a sonic anemometer and its application to heat and moisture fluxes. *Boundary-Layer Meteorology*, *26*(1), 81–93. https://doi.org/10.1007/BF00164332

Snedecor, G. W., & Cochran, W. G. (1989). *Statistical methods*. (8th ed., p. 502). Ames, IA: Iowa State University Press.

Sonntag, D. (1990). Important new values of the physical constants of 1986, vapour pressure formulations based on the ITS-90, and psychrometer formulae. *Zeitschrift für Meteorogie*, *40*(5), 340–344.

Taiz, L., Zeiger, E., Moller, I. M., & Murphy, A. (2014). *Plant physiology and development*. (6th ed., p. 888). Oxford University Press.

Wallace, J. M., & Hobbs, P. V. (2006). *Atmospheric science: An introductory survey* (p. 350). London: Academic Press.

Wang, X., Wang, C., Guo, Q., & Wang, J. (2016). Improving the CO_2 storage measurements with a single profile system in a tall-dense-canopy temperate forest. *Agricultural and Forest Meteorology*, *228–229*, 327–338. https://doi.org/10.1016/j.agrformet.2016.07.020

Widén, B., & Majdi, H. (2001). Soil CO_2 efflux and root respiration at three sites in a mixed pine and spruce forest: Seasonal and diurnal variation. *Canadian Journal of Forest Research*, *31*(5), 786–796. https://doi.org/10.1139/x01-012

Wright, J. D., Johnson, A. N., & Moldover, M. R. (2003). Design and uncertainty for a PVTt gas flow standard. *Journal of Research of the National Institute of Standards and Technology*, *108*(1), 21–47. https://doi.org/10.6028/jres.108.0010.6028/jres.108.004

Yang, B., Hanson, P. J., Riggs, J. S., Pallardy, S. G., Heuer, M., Hosman, K. P., et al. (2007). Biases of CO_2 storage in eddy flux measurements in a forest pertinent to vertical configurations of a profile system and CO_2 density averaging. *Journal of Geophysical Research*, *112*(D20). https://doi.org/10.1029/2006JD008243

Zhou, X. H., Yang, Q. H., Zhen, X. J., Li, Y. B., Hao, G. H., Shen, H., et al. (2018). Recovery of the three-dimensional wind and sonic temperature data from a physically deformed sonic anemometer. *Atmospheric Measurement Techniques*, *11*(11), 5981–6002. https://doi.org/10.5194/amt-11-5981-2018